Journal of Applied Polymer Science

Effects of Solution Mixing Temperature on Dielectric Properties of PMMA/Pristine Bentonite Nanocomposites

A. Uğur Kaya,[1] Selahaddin Güner,[2] Kadir Esmer[3,4]

[1]Department of Physics, Kocaeli University, Faculty of Art & Science, Kocaeli 41380, Turkey
[2]Department of Chemistry, Kocaeli University, Faculty of Art & Science, Kocaeli 41380, Turkey
[3]Yeni Yuzyil University, Faculty of Engineering and Architecture, Topkapi Dr. Azmi Ofluoglu Campus, Istanbul 34010, Turkey
[4]Department of Physics, Marmara University, Faculty of Art & Science, Göztepe Campus Istanbul 34722, Turkey
Correspondence to: A. Uğur Kaya (E-mail: augurkaya@gmail.com or ugurk@kocaeli.edu.tr)

ABSTRACT: We examined the effects of mixing temperature on the dielectric properties of polymethylmethacrylate (PMMA)-pristine bentonite nanocomposites by using X-ray diffraction, FT-IR and dielectric spectroscopies. The samples were prepared during 8 hours at temperatures 265 K, 273 K, 281 K, 289 K and 298 K without any intercalative agent and the PMMA to pristine bentonite weight ratio was chosen as 1 : 10. It was observed that with decreasing the mixing temperatures, the permittivity decreases and the dielectric relaxation displaces towards the lower frequencies with the decrease of mixing temperatures. © 2013 Wiley Periodicals, Inc. J. Appl. Polym. Sci. **2014**, *131*, 39907.

KEYWORDS: clay; dielectric properties; X-ray

Received 28 February 2013; accepted 29 August 2013
DOI: 10.1002/app.39907

INTRODUCTION

In the last two decades, polymer (PMMM)/clay nanocomposites have been widely used in both academics and industrial studies. First, polymer/clay nanocomposites were investigated by Toyota Research Center in Japan.[1,2] Thermal and mechanical properties of these nanocomposites which are obtained using different clays and polymers have been studied widely.[2–9]

To prepare polymer-clay nanocomposites, commonly used layered silicates belong to the same general family of 2 : 1 layered or phyllosilicates. The layer thickness is around 1 nm, and the lateral dimensions of these layers may vary from 30 nm to several microns. Stacking of the layers leads to a regular Van der Waals gap between the layers called the interlayer or gallery.[3]

Na–Bentonite clay which is one of the most used layered silicates in literature belongs to smectite group of the clay minerals. These clays are organized as platelets of micrometer size, made of two-dimensional tetrahedral (T) sheet of SiO_4 units linked by an octahedral (O) sheet Al(O,OH)6 units, forming T-O-T layers separated by an interlayer space of varying thickness. On the basal plane of the clay layers, oxygen atoms form a hexagonal network.[10]

With good mechanical and optical properties, Polymethylmethacrylate (PMMA) is one of the most commonly used acrylate polymers. This polymer was used with different clay to prepare PMMA/Clay nanocomposites. PMMA/Clay nanocomposites have been prepared by *in situ*,[11–13] suspension,[14,15] emulsion[16–18] polymerization, solution mixing,[19,20] and melt processing.[21–23] Solution mixing or solvent casting method is used to prepare intercalated structures of the polymer or clay as host material.[24,25]

In our previous study, it was seen that dielectric properties were directly affected from adsorption temperatures above the 298 K.[26] In this article, we work on dielectric properties of pristine bentonite/PMMA nanocomposites prepared at low temperatures below the 298 K. At the temperature below the 298 K, water content of the clay can be reduced and this reduce affects the adsorption and intercalation capability of clay. Therefore, the dielectric properties of polymer-clay nanocomposites can be changed. To observe the temperature effects on dielectric properties of nanocomposites, samples were prepared at five different mixing temperatures (265 K, 273 K, 281 K, 289 K, and 298 K) by solution mixing technique. FTIR and dielectric spectroscopy were used to obtain information about polymer/clay interactions. Furthermore, we have also employed the XRD technique as an additional supporting tool just to figure out polymer/clay interactions, namely, for observing swelling process between the clay layers.

EXPERIMENTAL

Materials

Pristine-bentonite, with cation exchange capacity (CEC) of 85 meq/100 g, was supplied by Eczacıbaşı Esan Co. (Istanbul-

TURKEY). PMMA was purchased from Aldrich with weight average molecular weight $M_w = 350{,}000$ g mol^{-1}. Chloroform (Fluka) was used as solvent.

Preparation of PMMA-Pristine Bentonite Nanocomposites

It was reported that increase of PMMA/MMT does not affect intercalation of PMMA molecules into clay galleries. It was also shown that mixing duration is not very important. It means that intercalation is a relatively fast process.[29] Therefore, pristine bentonite/PMMA ratio and mixing duration was chosen 10 : 1 (w : w) and 8 h respectively.

Totally, 100 mg PMMA was dissolved in 50 mL chloroform and 1 g pristine bentonite was added to the solution. Specially designed mechanical stirrer with round-bottom flask to mix solutions physically was immersed to the chiller and for each solution temperature; chiller temperature was set up and waited until stable. All solutions were mixed for 8 h with 120 rpm at 265K, 273 K, 281 K, 289 K, and 298 K, respectively. Suspensions were filtered and after the filtration, solid samples were dried for 24 h at room temperature.

Characterization of Materials

Totally, 10 mg pristine bentonite/PMMA sample was added to the 500 mg KBr. The mixture was blended in mortar. From this blended mixture, 200 mg was taken and pressed 6 ton to prepare FTIR pellets. FTIR spectra of pure pristine bentonite and pristine bentonite-PMMA nanocomposites were recorded on a Shimadzu 8201/86601 PC Infrared Spectrometer.

The X-Ray diffraction patterns of pristine bentonite and nanocomposites were determined using Cu Kα radiation with Rigaku X-Ray Diffractometer ($\lambda = 1{,}54$ A°, $2\theta = 2$–$20°$, with a resolution $0.02°2\theta$). Air moisture can affect the measurement. To prevent the air moisture effects, measurements were done same conditions for all samples with dry nitrogen flow.

Samples for dielectric measurements were formed as discs (pellets) with a diameter of 13 mm under a hydraulic press with 6 tons. Dielectric properties (i.e., capacitance, real and complex permittivity, tangent loss factor) were measured with a Wayne Kerr 6500 B Precision Impedance Analyzer at 1 V_{rms} potential.

RESULTS AND DISCUSSION

FTIR Studies

Pristine bentonite showed a characteristic peak at 1030 cm^{-1} corresponding to Si—O stretching (Figure 1). The peaks related to H-O-H bonds were observed near 3400 cm^{-1} and 1638 cm^{-1} for stretching and bending vibrations of absorbed water respectively. For samples (prepared at 265 K and 273 K), peaks observed near 3400 cm^{-1} were broadened and intensity of peaks were increased according to pure clay and the other samples . Peak at 3628 cm^{-1} is related to OH stretching vibrations of structural hydroxyl.[27] These peaks were broadened with decreasing mixing temperatures (Figure 2).

A Sharp peak at 1033 cm^{-1} is due to Si—O stretching frequency. Peak observed at 915 cm^{-1} is related to OH bending vibrations in dioctohedral 2 : 1 layer silicates. In Al-Mg-OH, OH vibration peak was observed at 842 cm^{-1}. At 791 cm^{-1}, it was observed OH vibration peak related to Mg-Fe-OH.

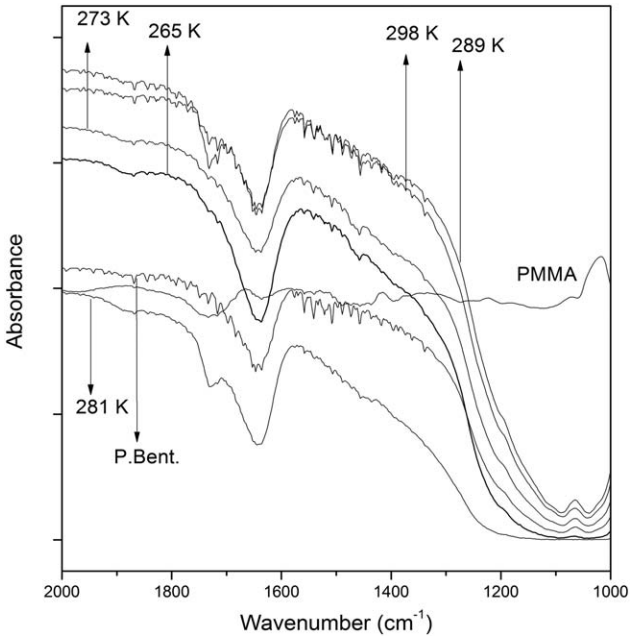

Figure 1. Infrared spectra of pristine bentonite, pure pmma and their nanocomposites prepared at different temperatures (2000–1000 cm^{-1})

Shoulder peak at 624 cm^{-1} is related to bending vibration of Si-O-Si.[27,28] Peaks observed at 1085 cm^{-1} and 470 cm^{-1} are related to amorphous silica (Figure 1).

It was observed interesting behavior at 1732 cm^{-1}. For samples prepared at 265 K and 273 K, shoulder appeared around 1732 cm^{-1} (C═O stretching) was weakened. C—H stretching peaks for PMMA between 2845 cm^{-1} and 2950 cm^{-1} were shifted to

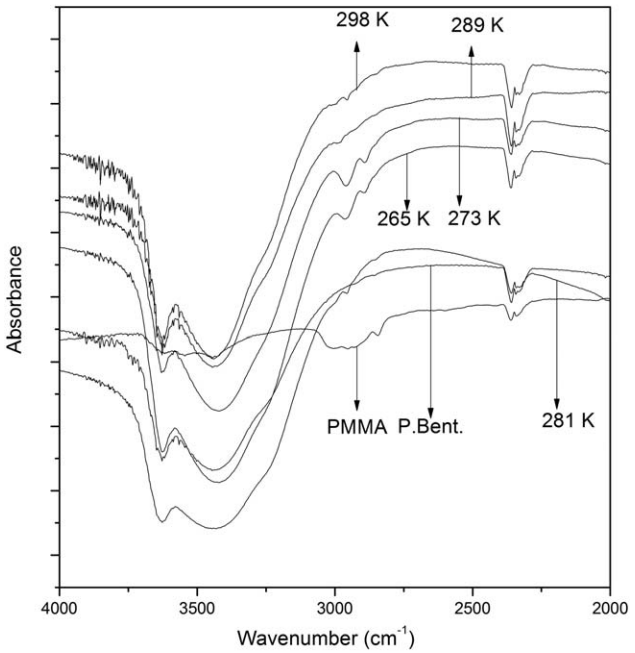

Figure 2. Detailed infrared spectra of pristine bentonite, pure pmma and their nanocomposites prepared at different temperatures (4000–2000 cm^{-1}).

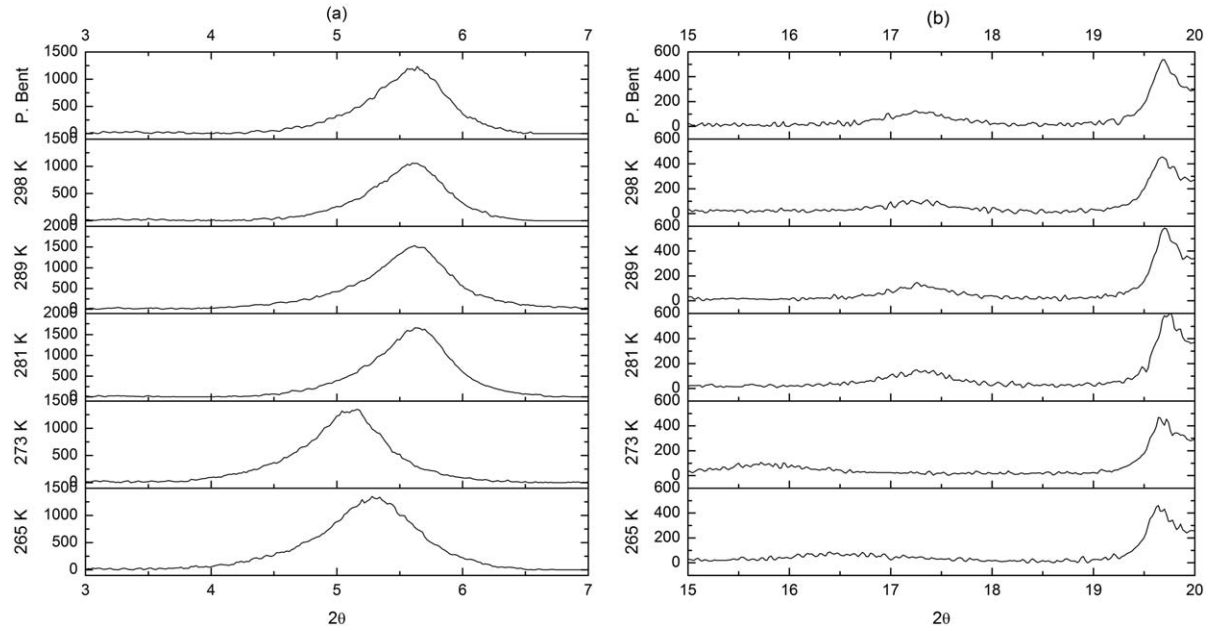

Figure 3. XRD plots of pristine bentonite and pristine bentonite-PMMA nanocomposites prepared at different temperatures (a) 3–7°, (b) 15–20°.

high wave numbers 2890 cm^{-1} and 2960 cm^{-1} for the samples prepared at 265 K and 273 K, respectively. For other samples prepared at 281 K, 289 K, 298 K, these peaks were weakened.

These results can be interpreted by weakness of the peaks at 1732 cm^{-1} for the samples prepared at 265 K and 273 K and near 3000 cm^{-1} for samples prepared at 281 K, 289 K, and 298 K. For samples prepared at 265 K and 273 K, weakness at 1732 cm^{-1} can be attributed to the interactions of PMMA molecules with the clay. Interactions between the carbonyl groups of PMMA and pristine bentonite may cause weakness of C═O stretching of PMMA.

On the other hand, CH stretching bands are weak compared to the C═O stretching. Therefore, for samples prepared at 281 K, 289 K, and 298 K, carbonyl peaks are more intense than CH stretching.

XRD Studies

Figure 3 shows the XRD plots of pristine bentonite and pristine bentonite-PMMA nanocomposites prepared at different temperatures. Table I shows the two theta and *d*-spacing values for three peaks on each sample. Pristine bentonite shows the characteristic basal peak at $2\theta=5.64°$ and *d*-spacing (001) is 15.66 Å. Other peaks were observed at 17.24° and 19.70°. It was shown that for the samples prepared at 265 K and 273 K, these basal peaks were shifted lower degrees and hence *d*-spacing were increased. This result is evidence of intercalation for these samples. On the other hand, the sample which prepared at 281 K has very close values to the pristine bentonite and for samples prepared at 289 K and 298 K increase of *d*-spacing is very small. It can be interpreted that for the samples prepared at 265 K and 273 K, intercalation can be dominant and for other samples prepared at temperatures 281 K, 289 K, and 298 K, adsorption may only be dominant but not strong. Increase of *d* spacing for samples prepared at 265 K and 273 K, show that more PMMA molecules can enter the galleries and the level of interactions between the polymer and pristine bentonite is high especially at edge of clay galleries.

It was reported that physical mixture of polymer-clay can not form a nanocomposite. This situation was observed for the samples prepared above the 273 K. In literature, intercalation was achieved by ion-exchange with cationic surfactants including primary, secondary, tertiary, and quaternary alkylammonium or alkylphosponium cations.[3] *d*-spacing of clay galleries can be increased readily with this cations or melt intercalation. Other study which was done by emulsion polymerization of PMMA in the presence of Na-montmorillonite does not include intercalative agent and shows 0.13 nm increase of *d*-spacing with PMMA 18.4 (wt %) as visitor on host montmorillonite. It

Table I. 2-theta and *d*-Spacing Values of Pristine Bentonite and Pristine Bentonite-PMMA Nanocomposites

Pristine Bentonite		265 K		273 K		281 K		289 K		298 K	
2θ	d(Å)	2θ	d(Å)	2θ	d(Å)	2θ	d(Å)	2θ	d(Å)	2θ	d(Å)
5.64	15.66	5.28	16.72	5.16	17.11	5.64	15.66	5.62	15.71	5.60	15.77
17.24	5.14	16.48	5.34	15.72	5.63	17.26	5.13	17.24	5.14	17.36	5.11
19.70	4.50	19.64	4.52	19.64	4.52	19.76	4.49	19.70	4.50	19.66	4.51

was also reported that *d*-spacing increase with increased PMMA content.[13]

In this study, although there were not either intercalative agents or melt intercalation methods, increase of *d*-spacing was about 0.15 nm. This increase can be attributed to the intercalation of the polymer to the clay galleries. This result can be explained by the swelling of silicate layers. It is well known that silicate layers can be swollen by solvents such as water, chloroform, or toluene. Clay is swollen in solvent and then polymer or polymer solution is added and mixed. Polymer chains intercalate between the clay layers with displacing the solvent.[29] In our study, while the solution was mixed, pristine bentonite could swell chloroform and then the polymer chains were displaced with chloroform and intercalate to the clay galleries.

Dielectric Studies

Dielectrical behavior is investigated with real (ε') and imaginary (ε'') parts of the dielectric constant ($\varepsilon^*=\varepsilon'+i\,\varepsilon''$). The real part ($\varepsilon'$) is related to deposited energy by external field and the imaginary part (dielectric loss) is related to loss of energy;

$$\varepsilon' = \frac{C_p}{C_0},\ \varepsilon'' = \varepsilon' \tan\delta \tag{1}$$

where, C_0: vacuum capacitance, C_p: capacitance, tanδ:loss factor.

Alternating current (ac) conductivity (σ^*) was calculated by;

$$\sigma^*(\omega)=\sigma'+j\sigma''=\omega\varepsilon_0\varepsilon''+j\omega\varepsilon_0\varepsilon' \tag{2}$$

where, ω: angular frequency, ε_0: free space dielectric constant, σ': real part and σ'' imaginary part of ac conductivity, respectively. Complex electric modulus $M^*(\omega)$ were determined by the following equations:

$$M^*(\omega)=\frac{1}{\varepsilon^*(\omega)}=M'+jM''=\frac{\varepsilon'}{\varepsilon'^2+\varepsilon''^2}+j\frac{\varepsilon''}{\varepsilon'^2+\varepsilon''^2} \tag{3}$$

where, M' and M'' are real and imaginer part of electric modulus, respectively.

Dielectric measurements were done by Wayne Kerr 6500 B Precision (20 Hz–5 MHz) Impedance Analyzer at 1 V_{rms} potential at room temperature. Figure 4 shows the variations of real part (permittivity) ε', imaginary part (dielectric loss) ε'' and tangent loss, respectively. It was reported that change in ε' values with decrease in frequency below 10^4 Hz represents the significant contribution of electrode polarization process.[35] In our study, the gradual decrease of real permittivity with the decrease in solution mixing temperatures represents decrease of electrode polarization effect [Figure 4(a)]. It was reported that water content of the clay can effect the electrode polarization at low frequencies.[36] Real permittivity decreases with decrease in water content of clay. Therefore, our results can be explained by the water uptake from the clay with decrease in solution mixture temperature.

Gradual decrease of dielectric loss (ε'') with decrease in solution mixing temperatures were observed [Figure 4(b)]. At high frequency region, the sample which was prepared at 265 K has the lowest dielectric loss values with respect to other samples [inset of Figure 4(b)]. In the medium frequency range, pristine bentonite and the sample prepared at 298 K show broad loss peaks. Loss Tangent of pristine bentonite (P. Bent.) and pristine bentonite-PMMA nanocomposites were given in Figure 4(c). It can be said that relaxations were slightly shifted to lower frequencies.

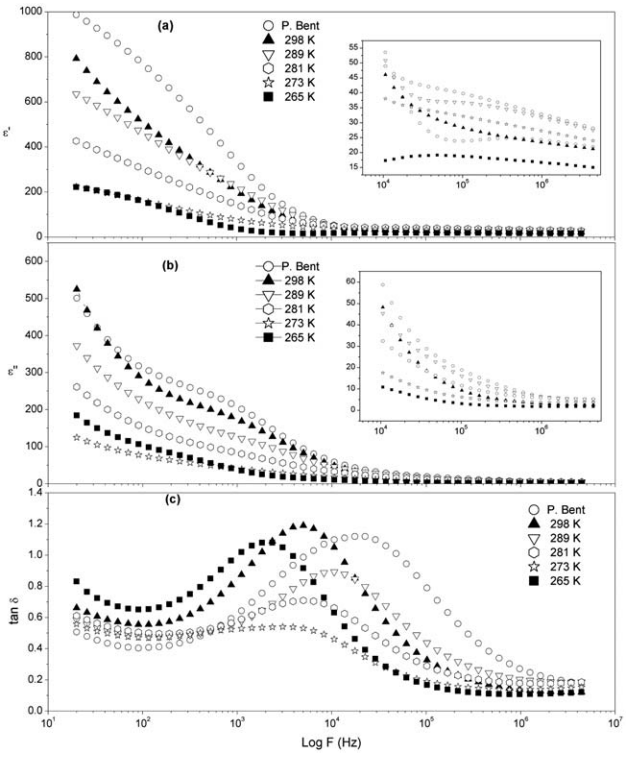

Figure 4. Real permittivity of pristine bentonite (P. Bent.) and pristine bentonite-PMMA nanocomposites (100–15 MHz).

Additional information can be extracted from the electric modulus. Electric modulus formalism can give some advantages to interpret relaxation phenomena. Large variation in the real and imaginer parts of the dielectric function at low frequencies can be minimized. Further, difficulties occurring from the electrode nature, the electrode-dielectric specimen contact, the injection of space charges and adsorbed impurities can be neglected.[37]

The M' and M'' spectra were given in Figure 5(a,b), respectively. The M' spectra of Pristine Bentonite-PMMA nanocomposites show the decrease in M' values with decrease in solution mixing temperature in the frequency region below the 10^4 Hz [Figure 5(a)]. Sharp peaks in M'' are shifted to the lower frequencies as the solution mixing temperature decreases [Figure 5(b)]. The electric modulus relaxation time is determined from loss peak frequency $f_p(M'')$ using the relation $\tau_M=\left(2\pi f_p(M'')\right)^{-1}$. The evaluated τ_M values were plotted against to solution mixing temperature (Figure 6). It was observed that relaxation time increase with decrease in solution mixing temperature.

It was reported that shifting the relaxation frequency to the lower frequencies is related to the water content of the clay.

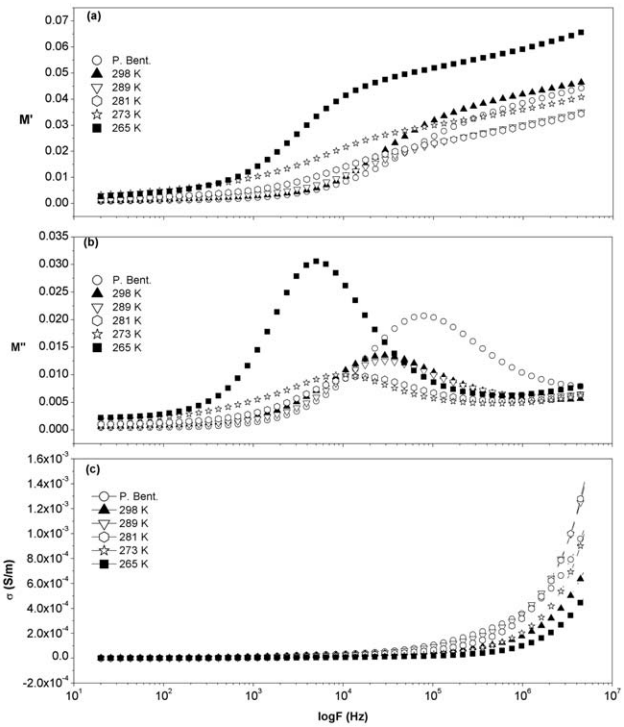

Figure 5. Real permittivities of pristine bentonite (P. Bent.) and pristine bentonite-PMMA nanocomposites (10^5-10^7Hz).

Relaxations observed at lower frequency are attributed to the total conductivity of the clay samples. The high frequency relaxation peak, observed in modulus presentation at $f>10^5$ Hz is related to the polarization of bound water.[33] Another study, which is the polymer host and the clay is visitor shows high frequency peak in the electric modulus due to reoriented dynamics of polar groups of the polymer. It has been also reported that

Table II. Parameters Obtained from Universal Power Law fit to the Experimental Data of Pristine Bentonite and Pristine Bentonite-PMMA Nanocomposites

Pristine bentonite and nanocomposites	σ_{dc} (μS/m)	A (10^{-9})	n
P. Bentonite	8.03	0.67	0.62
298 K	14.2	1.32	0.85
289 K	13.1	4.05	0.82
281 K	9.99	0.99	0.92
273 K	5.55	0.22	0.99
265 K	3.55	0.08	1.01

increase in relaxation time is evidence of the increase in hindrance to the polymer chain.[37] In present study, low dielectric constants and shifting the relaxation peaks to the lower frequency with decrease in solution mixing temperature can be explained by the water uptake from the clay.

The σ' spectra of pristine bentonite and pristine bentonite-PMMA nanocomposites were given in Figure 5(c). All the samples have frequency independent plateau which correspond to ionic or dc electrical conductivity σ_{dc} and dispersion at higher frequencies (above 10^4Hz). This behavior obeys the power law $\sigma^*(\omega)=\sigma_{dc}+A\omega^n$, where A is the pre-exponential factor and n is the fractional exponent (ranging between 0 and 1 for the electrolyte).[38] The solid line in σ'spectra denotes fit of experimental data to the power law expression. σ_{dc}, A and n values of power law expression were given in Table II. It can be seen that the dc conductivity values of nanocomposites decrease with decrease in solution mixing temperature (Figure 7). Especially, for the samples which were prepared at 265 K and 273 K have lower dc conductivity values with respect to dc conductivity of

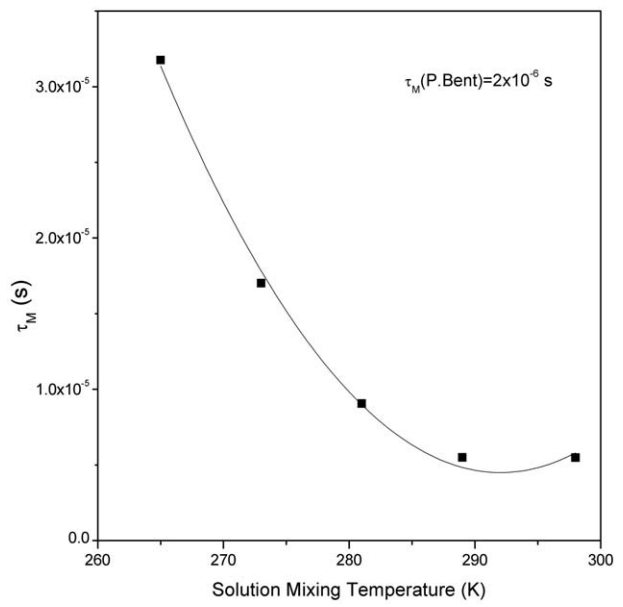

Figure 6. Loss factors of pristine bentonite (P. Bent.) and pristine bentonite-PMMA nanocomposites.

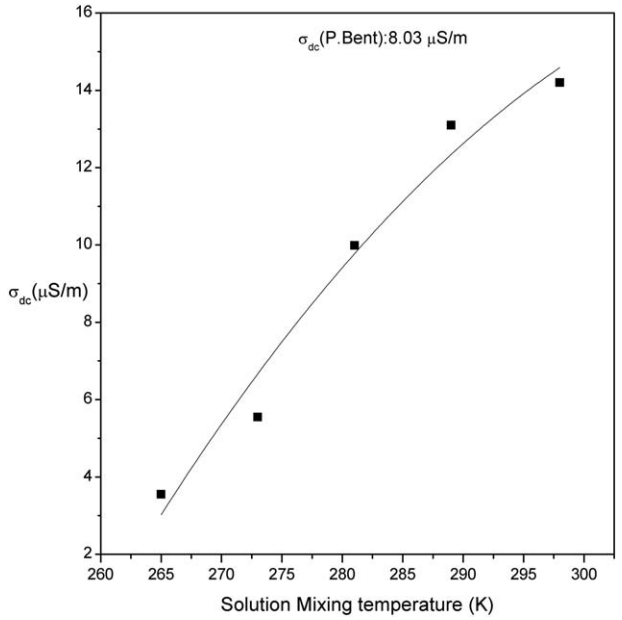

Figure 7. AC conductivity of pristine bentonite (P. Bent.) and pristine bentonite-PMMA nanocomposites.

pristine bentonite whereas the samples which were prepared at 281 K, 289 K, and 298 K have higher values. This lower dc conductivity values with decrease in solution mixing temperature can be attributed the decrease in water content of the clay which reduces electrode polarization effect. Water uptake can occur not only on the surface of the clay but also in the clay galleries. Especially, for the samples (265 K an 273 K), water uptake can occur both on the surface of the clay and in the clay galleries. This result can be supported by the increase in *d*-spacing values of these samples. Therefore it can be concluded that water uptake from the clay galleries can cause strong electrostatic attraction between the gallery cations and clay plates. This strong electrostatic attraction reduces the ion mobility. Therefore lower σ_{dc} values in the samples 265 K and 273 K with respect to other samples can be explained by reduced ion mobility. Similar result was reported by Kaviratna's group.[36]

On the other hand, increase in *d*-spacing of the clay galleries by intercalation of the polymer molecules into the clay galleries is important evidence to explain the decrease of real permittivity. It was shown that increased interlayer spacing decrease the dielectric constant.[29,30,35,37] In those studies, to produce polymer-clay nanocomposites, PMMA is host and clay is visitor and clay was used with modifier. It was reported that the dipole orientation of the polar side of PMMA was constrained because of confinement and interference of clay.[30]

In our study, the clay is host and PMMA is visitor in the ratio 10 : 1(w : w). The intercalation of PMMA molecules into pristine bentonite galleries can be restricted the dipole orientation of the polymer and the clay. PMMA chains were intercalated into the clay galleries tightly. This intercalation was supported by weakness of the carbonyl peaks in the FTIR spectra.

It was reported that main driving force between polymer and clay results from an orientation of the polymer chain, forming hydrogen bonds with the hydroxylated surface of the clay.[31] Therefore, it can be said that surface interactions between the polymer and clay is more effective for samples prepared at 273K, 281 K, 289 K, and 298 K with respect to the other sample. Otherwise, for sample prepared at 265 K, polymer can try to enter clay galleries instead of adsorb to the clay surface. Therefore, decrease in real permittivity for sample prepared at 265 K according to pure clay and other samples can be explained by this tight intercalation (inset of Figure 4).

From the results discussed above, it should be explained the mechanism of the water uptake from the clay structure. It was reported the individual H_2O molecules are bonded stronger than in unbound liquid but weaker than in solid form.[32] At higher temperatures than the room temperature, relaxations frequencies slightly shifted to lower frequency. This result was explained by the evaporation of water molecules from surface of the clay.[33] It was also reported that relaxation peaks shifted to lower frequencies and ε' decrease with reduction of water content of the clay.[34] From the reports described above, it can be said that water molecules at the surface of the clay can leave at lower temperature than 273 K and at higher temperature than the room temperature. In this study, remove of water molecules from the surface of the clay at lower temperature than 273 K, can cause lower real permittivity and shifting of relaxation peaks to the lower frequencies according to the samples prepared at 281 K, 289 K, and 298 K. Therefore reduce in dielectric constants and slide of relaxation peaks to the lower frequencies with decrease in solution mixing temperatures can be explained by two ways: First, increase in *d*-spacing of pristine bentonite galleries with intercalation of PMMA molecules into the pristine bentonite galleries can constrain the dipole orientation of both polar side of pristine bentonite and polymer. Second, removing of water molecules at lower preparation temperatures (below 273 K) can decrease the polymer-clay interactions molecules on the surface of the clay.

CONCLUSIONS

We have studied PMMA-pristine bentonite nanocomposites prepared by solution mixing method at different temperatures. It was observed that the samples prepared at temperatures 265 K and 273 K exhibit the intercalation of PMMA into the pristine bentonite galleries. The XRD measurements have shown the increase in *d*-spacing of the pristine bentonite by decreasing the temperature. These results show that the weakness of the carbonyl group peaks in FTIR spectra can be interpreted in favor of the intercalation as well. It was also observed that the intercalation constrains the dipole orientations and results in the decrease of the dielectric constants. The decrease in the value of dielectric constants as well as the shift of the relaxation peaks towards the lower frequencies, with decreasing the mixing temperatures, can be explained in two ways: (i) The intercalation of PMMA molecules into the pristine bentonite galleries restricts the orientations of dipoles. (ii) The disappearance at lower preparation temperatures (below 273 K) of water molecules from the surface of the clay results in the decrease of the polymer-clay interactions. At lower frequency region (below 10^4 Hz), electrode polarization effect decrease with decrease in solution mixing temperature. DC conductivity values of nanocomposites decrease with decrease in solution mixing temperature. Relaxation time (τ_M) increases with decrease in the mixing temperature.

In summary, it seems that with the low mixing temperature near 273 K, it may be possible to produce intercalated polymer-clay nanocomposites in the absence of an intercalative agent.

ACKNOWLEDGMENTS

This work was supported by Kocaeli University Scientific Research Center Fund 2012-34- HDP. We also thank to Eczacıbaşı Esan Co. Istanbul for Pristine Bentonite supply.

REFERENCES

1. Okada, A.; Kawasumi, M.; Kurauchi, T.; Kamigaito, O. *Polym. Prepr.* **1987**, *28*, 447.
2. Kojima, Y.; Usuki, A.; Kawasumi, M.; Okada, A.; Fukushima, Y.; Karauchi, T.; Kamigaito, O. *Mater. Res. J.* **1993**, *8*, 1185.
3. Ray, S.S.; Okamoto, M. *Prog. Poly. Sci.* **2003**, *28*, 1539.
4. Giannelis, E. P. *Adv. Mater.* **1996**, *8*, 29.

5. Aranda, P.; Ruiz-Hitzky, E. *App. Clay Sci.* **1999**, *15*, 119.
6. Gilman, J. W. *App. Clay Sci.* **1999**, *15*, 31.
7. LeBaron, P. C.; Wang, Z.; Pinnavaia, T. *J. App. Clay Sci.* **1999**, *15*, 1129.
8. Seçkin, T.; Gültek, A.; İçduygu, M. G.; Önal, Y. *J. Appl. Polym. Sci.* **2002**, *84*, 164.
9. Younghoon, K.; White, J. L. *J. Appl. Polym. Sci.* **2005**, *96*, 1888.
10. Keller-Besrest, F.; Benazeth, S.; Souleau, C. *Mater. Lett.* **1995**, *24*, 17.
11. Xie, G.; Yang, G.; Fang, X.; Ou, Y. *J. Appl. Polym. Sci.* **2003**, *89*, 2256.
12. Jash, P., Wilkie, C. A. *Polym. Degrad. Stabil.* **2005**, *88*, 401.
13. Qu, X.; Guan, T., Liu, G.; She, Q.; Zhang, L. *J. Appl. Polym. Sci.* **2005**, *97*, 348.
14. Choi, Y. S.; Ham, H. T.; Chung, T. *J. Polymer* **2003**, *44*, 8147.
15. Zhao Q.; Samulski, T. *Macromolecules* **2005**, *38*, 7967.
16. Lee, D. C.; Jang, L. W. *J. Appl. Polym. Sci.* **1996** *61*, 1117.
17. Huang, X.; Brittain, W. *J. Macromol.* **2001**, *34*, 3255.
18. Yeh, J.; Liou, S., Lai; M., Chang, Y.; Huang, C.; Chen, C.; Jaw, J.; Tsai, T.; Yu, Y. J. *J. Appl. Polym. Sci.* **2004**, *94*, 1936.
19. Hwu, J. W.; Jiang, G. T.; Gao, Z. M.; Xie, W.; Pan, W. P. *J. Appl. Polym. Sci.* **2002**, *83*, 1702.
20. Xu, Y.; Brittain, W. J.; Xue, C.; Eby, R. K. *Polymer* **2004**, *45*, 3735.
21. Kumar, S.; Jog, J. P.; Natarajan, U. *J. Appl. Polym. Sci.* **2003**, *89*, 1186.
22. Shen, Z.; George, S. P.; Cheng, Y. *J. Appl. Polym. Sci.* **2004**, *92*, 2101.
23. Tiwari, R. R.; Natarajan, U. *J. Appl. Polym. Sci.* **2007**, *105*, 2433.
24. Hyun, Y. H.; Lim, S. T.; Choi, H. J.; Jhon, M. S. *Macromolecules* **2001**, *34*, 8084.
25. Lim, S. K.; Kim, J. W.; Chin, I.; Kwon, Y. K.; Choi, H. *J. Chem. Mater.* **2002**, *14*, 1989.
26. Kaya, A. U.; Esmer, K.; Tekin, N.; Beyaz, S. K. *J. Appl. Polym. Sci.* **2011**, *120*, 874.
27. Madejova, J. *Vibrational Spectroscopy* **2003**, *31*, 1.
28. Tyagi, B.; Chudasama, C. D.; Jasra, R. V. *Spectrochim Acta A* **2006**, *64*, 273.
29. Huskic, M.; Zigon, M. *J. Appl. Polym. Sci.* **2009**, *113*, 1182.
30. Wang, H. W.; Shieh, C. F.; Chang, K. C.; Chu, H. C. *J. Appl. Polym. Sci. 97*, 2175.
31. Sengwa, R. J.; Sankhla, S.; Choudhary, S. *Ionics* **2010**, *16*, 697.
32. Sjöström, J.; Swenson, J.; Bergman, R.; Kittaka, S. *J. Chem. Phys.* **2008**, *128*, 154503.
33. Saltas, V.; Vallianatos, F.; Triantis, D. *J. Non-Crystalline Solids* **2008**, *354*, 5533.
34. Stillman, D. E.; Grimm, R. E.; Dec, S. F. *J. Phys. Chem. B* **2010**, *114*, 6065.
35. Choudhary, S.; Sengwa, R. *J. Ionics* **2011**, *17*, 811.
36. Kaviratna, P. D.; Pinnavaia, T. J.; Schroeder, P. A. *J. Phys. Chem. Solids* **1996**, *57*, 1897.
37. Sengwa, R. J.; Choudhary, S.; Sankhla, S. *Comp. Sci. Tech.* **2010**, *70*, 1621.
38. Jonscher, A. K. Dielectric Relaxation in Solids; Chealse Dielectric Press, **1983**.